

---

---

# Optical Parametric Oscillators in Lidar Sounding of Trace Atmospheric Gases in the 3–4 $\mu\text{m}$ Spectral Range

O. A. Romanovskii<sup>a, b</sup>, S. A. Sadovnikov<sup>a</sup>, O. V. Kharchenko<sup>a</sup>,  
V. K. Shumsky<sup>a</sup>, and S. V. Yakovlev<sup>a, b</sup>

<sup>a</sup>*V.E. Zuev Institute of Atmospheric Optics, Siberian Branch, Russian Academy of Sciences, Tomsk, Russia*

<sup>b</sup>*National Research Tomsk State University, Lenin Ave. 36, Tomsk, 634050 Russia*

*e-mail: roa@iao.ru*

Received in final form, January 20, 2016

**Abstract**—Applicability of a KTA crystal-based laser system with optical parametric generation to lidar sounding of the atmosphere in the spectral range 3–4  $\mu\text{m}$  is studied in this work. A technique developed for lidar sounding of trace atmospheric gases is based on differential absorption lidar (DIAL) technique and differential optical absorption spectroscopy (DOAS). The DIAL-DOAS technique is tested to estimate its efficiency for lidar sounding of atmospheric trace gases.

**Keywords:** atmosphere, lidar sounding, DIAL, DOAS, trace gases, nonlinear crystal

**DOI:** 10.3103/S1060992X16020041

## 1. INTRODUCTION

The development of noncontact laser methods for environmental diagnostics (atmosphere and ocean) requires lasers capable of generating radiation in a certain preset wavelength range with a small frequency step. Common up-to-date differential absorption lidars allow measuring only several atmospheric gases. High-power radiation sources used in them, such as CO<sub>2</sub> and DF (HF) lasers, have a limited number of coincidences of lasing lines with atmospheric gas absorption lines [1], and do not allow in principle a simultaneous temporal and spectral analysis of multifrequency response of the atmosphere because of a need for frequency turning. IR Fourier-transform gas analyzers are free of this disadvantage; however, low-power thermal radiation sources are used in them due to the lack of high-power broadband sources of coherent radiation. They allow only integral measurements along measuring paths of up to several hundreds of meters with the use of special reflectors.

Up-to-date radiation sources used in solution of atmospheric problems are based on IR broadband molecular lasers and parametric frequency converters on the basis of nonlinear crystals, which allow overlapping the range 2–18  $\mu\text{m}$  by means of generation of overtones, harmonics, and summation and difference laser frequencies. To overlap the near- and middle IR region, radiation of optical parametric oscillators (OPO) on the basis of nonlinear crystals is often used [1, 2].

Ground-based and aircraft differential absorption (DIAL) measurements were used for vertical profiling of ozone in the troposphere and stratosphere [3–6] and tropospheric water vapor [7], for mapping strong ethane and NO<sub>2</sub> pollution of the surface air layer, and for determining the NO<sub>2</sub> horizontal distribution in diesel vehicle emissions [8]. The DIAL can be also used in lidar sounding of meteorological parameters of the atmosphere [9].

However, laser radiation is required to be monochromatic in the standard DIAL technique. A wide spectral profile of the laser radiation decreases the effective absorption coefficient, which decreases the measurement sensitivity. Finally, the problem of standard DIAL measurements (especially of tropospheric ozone) at only two radiation wavelengths means that the disturbing absorption (by foreign gases, e.g., nitrogen dioxide) is ignored, which results in errors introduced by a priori uncertain absorption coefficients.

These disadvantages are absent in the differential optical absorption spectroscopy (DOAS) [10–13]. DOAS allows spectrally resolved measurements in a broad band, which provides for identification of several gases even in the case of overlapping absorption bands. Another advantage of the technique is independence of aerosol and molecular scattering due to the filtration of high frequencies used for the spectral

measurements. However, DOAS capabilities for vertical profiling are restricted; only path-average measurements have been carried out by now.

A technique which combines advantages of both methods—spatial resolution of the DIAL technique and identification of gases in DOAS—could be a promising approach to solution of the problem. The new technique uses broadband radiation and a CCD detector, which ensures measurement of backscattering signals with simultaneous altitude and wavelength resolution.

The aim of this work is the development of a technique for lidar sounding of trace atmospheric gases (TAGs), which combines DIAL and DOAS, and its validation in a numerical experiment for estimation of capabilities of lidar sounding of the gas composition of atmosphere in the 3–4  $\mu\text{m}$  spectral range with an OPO-based laser system.

## 2. DIAL AND DOAS TECHNIQUE FOR LIDAR TAG SOUNDING

The main principle of operation of a DIAL lidar consists of the fact that a part of backscattered laser radiation is transformed by molecules and aerosol particles when propagating through the atmosphere. A laser beam is attenuated (according to the Lambert-Beer law) due to the molecular absorption and molecular and aerosol scattering. That is, a signal detected is a function of this attenuation, the fraction of backscattered photons, path length, and laser radiation power. The  $P_R$  signal from a scattering layer of  $\Delta z$  in thickness can be represented as

$$P_R(z, \lambda) = P_0(\lambda) \frac{A_D}{z^2} \eta(\lambda) O(z) \Delta z \beta(z, \lambda) e^{-2\tau(z, \lambda)}, \quad (1)$$

where  $P_0(\lambda)$  is the laser radiation power,  $A_D$  is the instrumental function width,  $O(z)$  is the overlapping region of the laser beam and detector's field-of view,  $\beta(z, \lambda)$  is the mass coefficient of backscattering radiation,  $\eta(\lambda)$  is the efficiency of the receiving-transmitting system,  $\Delta z$  is the spatial resolution along the sounding path, and  $\tau(z, \lambda)$  is the attenuation coefficient.

The DIAL technique consists in calculation of the atmospheric gas concentration by the difference in lidar signals at on- and off-wavelengths with different molecular absorption. The concentration of a gas under study is calculated by the equation

$$n(z) = \frac{1}{2\Delta\sigma_{\text{abs}}\Delta z} \ln \left( \frac{P_R(z, \lambda_{\text{on}})P_R(z + \Delta z, \lambda_{\text{off}})}{P_R(z, \lambda_{\text{off}})P_R(z + \Delta z, \lambda_{\text{on}})} \right), \quad (2)$$

where  $\sigma_{\text{abs}}$  is the absorption cross section.

This equation is true only if the disturbing absorption by other gases is weak and the scattering properties of aerosol particles do not change in the ranges  $\Delta\lambda$  and  $\Delta z$ . The disturbing absorption and inhomogeneities of the aerosol layer results in high errors of gas profiling.

Disadvantages of the DIAL technique are caused by uncertainties of a priori absorption coefficients at two (three) wavelengths. DOAS allows avoiding these disadvantages, monitoring the transmission in the UV, visible and IR regions in a broad band (20–100 nm). In DOAS, the structured molecular absorption (on about several nanometers in width) is separated from the Lambert-Beer scattering, which is almost independent of the wavelength and can be eliminated using a high-frequency filter. In addition, several absorbing gases can be measured simultaneously by (least square) fitting the calculated molecular absorption to the observed one. The use of absorption measured at several wavelengths solves the problem.

The first step in DOAS is the calculation of the ratio of the spectrum observed ( $I_{\text{OBS}}$ ) to the reference spectrum ( $I_{\text{REF}}$ ), which is found from the laser spectrum ( $I_0$ ) measured with the same detector. An atmospheric spectrum at a known content of absorbing gases can be used as  $I_{\text{REF}}$ . Calculating the ratio ( $I_{\text{OBS}}/I_{\text{REF}}$ ) and taking its natural logarithm, the optical depth can be found:

$$-\ln \left( \frac{I_{\text{OBS}}}{I_{\text{REF}}} \right) = \sum_i \sigma_{\text{abs}}^i ([n_i(z)]_{\text{OBS}} \Delta z_{\text{OBS}} - [n_i(z)]_{\text{REF}} \Delta z_{\text{REF}}) + Y(\beta). \quad (3)$$

Equation (3) includes the wavelength-dependent absorption (the first term in Eq. (3)) and the scattering  $Y(\beta)$ , which is mainly determined by the backscattering coefficient  $\beta$ .

The ratio is independent of the laser radiation spectrum or the spectral dependence of the receiving optics, spectrometer, and detector, which is an important advantage of DOAS. The so measured magnitude is equal to the difference in the concentration of absorbing gases in the reference case and in the case of real atmosphere.

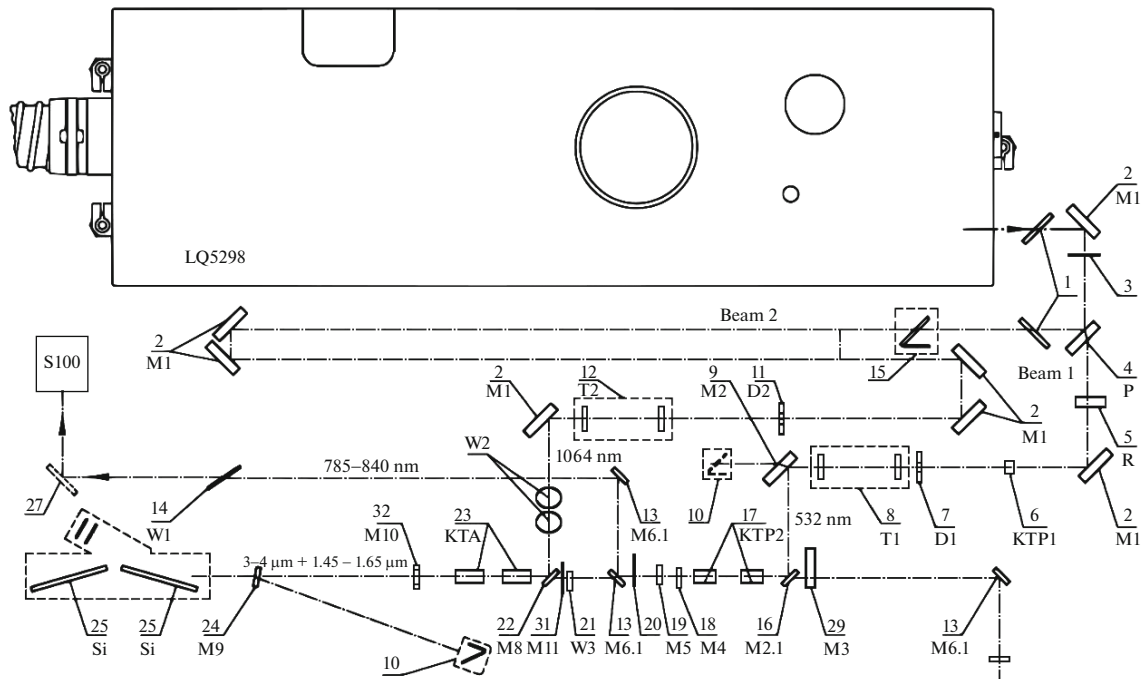


Fig. 1. Optical diagram of the laser system.

The weakly variable scattering  $Y(\beta)$  is eliminated using a high-frequency filter and different approaches. The simplest of the approaches is the use of a second- or third-order polynomial, which is fitted to the difference in the optical depth and then eliminated, leaving the so-called differential spectrum or differential optical depth. We should emphasize that this filtering process allows DOAS to overcome the problem of attenuation by unknown or ambiguously characterized scattering (aerosol or Rayleigh) typical for DIAL.

A differential spectrum is usually retrieved by several hundreds of points; the number of fitting parameters is no more than six. Thus, equation (2) becomes overdetermined and is solved with the least-square method. Under this approach, the fitting coefficients are varied for the fitting spectrum to match the best with the spectrum observed. In the general case, the method resolution corresponds to the molecular absorption under which the Lambert law fulfils. In this case, if the absorption coefficients are known, the integral content of each gas can be found. Simultaneous determination of the concentrations of several gases is an important advantage of DOAS as compared to the DIAL technique.

### 3. OPO LASER SYSTEM FOR REMOTE SOUNDING OF THE ATMOSPHERE

In this work, we consider a laser system (designed by SOLAR LS Company, Minsk) which is a part of a DIAL lidar and ensures the tunable generation of nanosecond radiation pulses in the 3–4  $\mu\text{m}$  range. A possibility of sounding some atmospheric gases along surface paths in the spectral range under study is estimated on the basis of the laser specifications.

Figure 1 shows the optical diagram of the laser system.

The system includes: temporary mirror (removable) for controlling the pulse energy at 1064 nm (1), rotating mirror M1 with high reflectivity for radiation at 1064 nm (2),  $\lambda/2$  retarder for 1064 nm (3), polarizer P (4),  $45^\circ$  quartz rotator R of radiation at 1064 nm (5), KTP1 crystal for the 2nd harmonic generation (6), aperture diaphragm D1,  $\varnothing 6$  mm (7), telescope T1,  $\times 1.8$  (8), dichroic mirror M2 with high reflectivity for radiation at 532 nm (9), laser radiation trap (10), aperture diaphragm D2,  $\varnothing 7$  mm (11), telescope T2,  $\times 1.5$  (12), dichroic mirror M6.1 with high reflectivity for radiation at 785–840 nm (13), shielding window (14), (removable) laser radiation trap (15), dichroic mirror M2.1 with high reflectivity for radiation at 532 nm (16), KTP2 crystals for OPO (17), output mirror M4 semitransparent for radiation at 785–840 nm (18), return mirror M5 with high reflectivity for radiation at 532 nm (19),  $\lambda/2$  retarder for the 1450–1650 nm range (20), IRS7 glass shielding window (21), dichroic mirror M8 with high reflectivity for radiation at

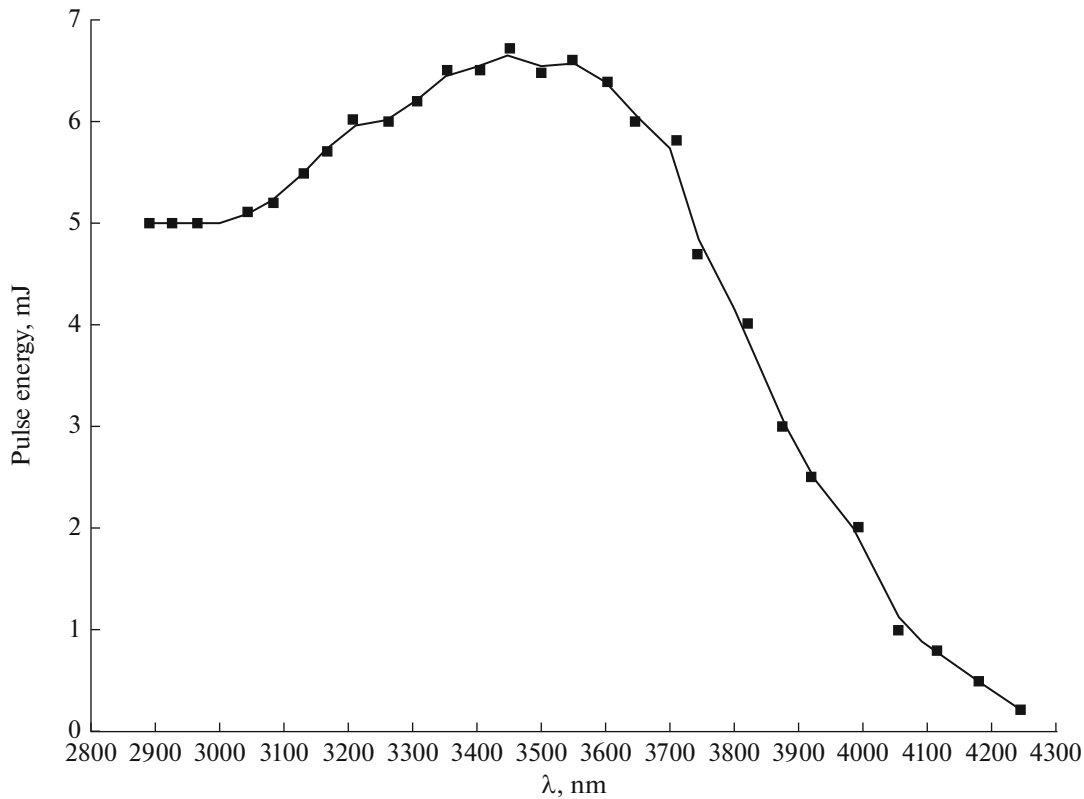


Fig. 2. Tuning curve of KTA-based OPO in the 3–4  $\mu\text{m}$  range.

1064 nm (22), KTA crystals for the high-power OPO (23), dichroic mirror M9 with high reflectivity for radiation at 1064 nm (24), Si plate (25), glass plate (27), temporary dichroic mirror (removable) with high reflectivity for radiation at 1450–1650 nm (28), Ag-coated totally reflecting mirror M3 (29), totally reflecting mirror M11 with high reflectivity for radiation at 1450–1650 nm (31), and output mirror M10 semitransparent for radiation at 1450–1650 nm (32).

Figure 2 shows the tuning curve of a KTA-based OPO. It is seen that its output pulse energy is quite high in the 3–4  $\mu\text{m}$  range (the curve attains a peak of > 6 mJ).

Tables 1 and 2 present main specifications of the pumping laser and radiation converter.

In the main, the laser system includes:

- LQ529B Nd:YAG pulsed laser;
- radiation converter with the wavelength tuning range 3–4  $\mu\text{m}$ ;
- step motor (SM) control of the wavelength;
- SM controller;
- S100 spectrometer;
- Common base for the laser and converter with a system for guiding pumping radiation in the converter.

**Table 1.** Specifications of LQ529B pumping laser

Pulse frequency	10 Hz
Output energy: at 1064 nm	350 mJ
Pulse length at 1064 nm, FWHM	10–13 ns
Beam diameter at 1064 nm	$\leq 6$ mm
Beam divergence at 1064 nm	$\sim 1.5$ mrad
Stability of pulse energy at 1064 nm, better than	$\pm 2.5\%$

**Table 2.** Specifications of radiation converter

Wavelength tuning range	3–4 $\mu\text{m}$
Radiation line width	$<5 \text{ cm}^{-1}$
Pulse energy, in the tuning curve peak	$>5 \text{ mJ}$
Pulse frequency	10 Hz
Radiation divergence	$</= 2 \text{ mrad}$
Wavelength tuning control	with 3 SMs

**Table 3.** Input data for numerical simulation of laser sounding

Lidar system parameter	Parameter value
Receiver area $A_{\text{rec}} (D = 0.3 \text{ m})$	$7 \times 10^{-8} \text{ km}^2$
Instrumental function width	$1 \text{ cm}^{-1}$
Receiving system efficiency	0.3
Spatial resolution $\Delta R$	1 km
Pulse energy maximum	5 mJ
Pulse frequency	10 Hz
Pulse length	10–13 ns
Radiation divergence	2 mrad
Tuning range of the laser	3–4 $\mu\text{m}$
Aerosol backscattering coefficient $\beta_{\pi}$	$2.3 \times 10^{-3} \text{ km}^{-1}$
Photodetector NEP	$1 \times 10^{-9} \text{ W}$

**Table 4.** Informative wavelengths chosen for TAG sounding in the 3–4  $\mu\text{m}$  region by DIAL-DOAS technique

Gas	$\lambda_{\text{abs}}, \mu\text{m}$ (in air)	$\nu_{\text{abs}}, \text{cm}^{-1}$ (in air)	$T_{\text{gas}}$	$T_{\text{dist}}$
HBr	3.98730	2507.962	0.79	0.99
HCl	3.57191	2799.622	0.60	0.93
N <sub>2</sub> O	3.87664	2579.55	0.85	0.90
NO <sub>2</sub>	3.42577	2919.051	0.73	0.89

The DIAL-DOAS technique developed for TAG measurements was validated for estimation of the lidar signal levels, using the specifications of the above described KTA-based OPO laser system.

#### 4. SIMULATION OF TAG LIDAR MEASUREMENTS IN THE 3–4 $\mu\text{m}$ RANGE

Sounding of some atmospheric gases (HCl, HBr, NO<sub>2</sub>, and N<sub>2</sub>O) along surface atmospheric paths (in the range 1–5 km) has been numerically simulated. The standard midlatitude summer model was used in the simulation. The disturbing absorption of all main atmospheric gases was considered; the HCl, HBr, and NO<sub>2</sub> concentrations were taken equal to 1 ppm (at background atmospheric concentrations of 1 ppb, 1 ppb, and 3.7 ppb, respectively), and the N<sub>2</sub>O concentration, to 1.5 ppm (at a background concentration of 0.3 ppm). Input data for the numerical simulation are given in Table 3.

Table 4 represents the information-bearing wavelengths used in the numerical simulation and appropriate for DIAL-DOAS sounding of the TAGs under study.

Spatially and spectrally resolved lidar echo signals in the TAG wavelength range, given in Table 4, calculated for surface tropospheric paths are shown in Fig. 3a, b for N<sub>2</sub>O and NO<sub>2</sub>, respectively, and in Fig. 4a, 4b, for HBr and HCl, respectively.

Figures 3 and 4 show that the level of lidar echo signals exceed the level of photodetector noise equivalent power (NEP =  $10^{-9} \text{ W}$ ) in the whole altitude range under study (0–5 km).

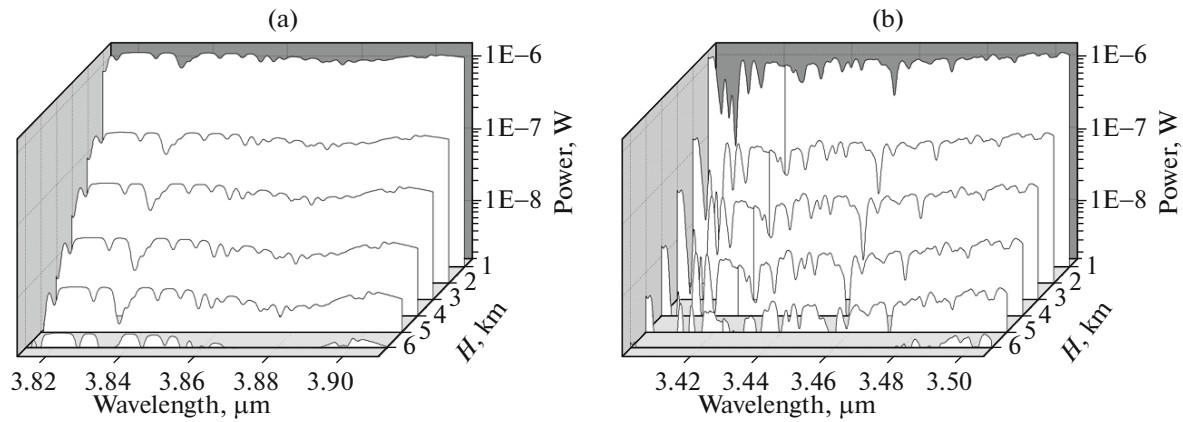


**Fig. 3.** Spatially and spectrally resolved lidar echo signals of (a)  $\text{N}_2\text{O}$  and (b)  $\text{NO}_2$  sounding in the region of KTA-based OPO operation (instrumental function width is  $1\text{ cm}^{-1}$ ).

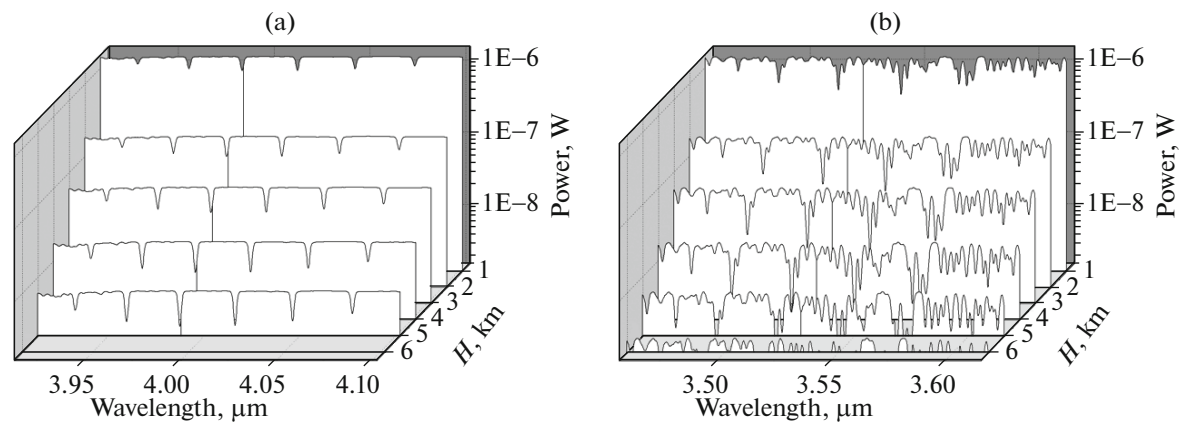


**Fig. 4.** Spatially and spectrally resolved lidar echo signals of (a)  $\text{HBr}$  and (b)  $\text{HCl}$  sounding in the region of KTA-based OPO operation (instrumental function width  $1\text{ cm}^{-1}$ ).

The numerical simulation results show a possibility of retrieving lidar signals along paths up to 5 km long during sounding of  $\text{N}_2\text{O}$  and  $\text{NO}_2$ , as well as  $\text{HCl}$  and  $\text{HBr}$ , with KTA-based OPO radiation in the 3–4  $\mu\text{m}$  range.

## 5. CONCLUSIONS

The technique developed for lidar sounding of TAGs, which combines DIAL and DOAS, and its validation in numerical experiments confirm prospects of the use of the selected information-bearing wavelengths for lidar sounding of the gas composition of the atmosphere in the 3–4  $\mu\text{m}$  range with an OPO-based laser system. The numerical simulation performed shows that a KTA-based OPO laser is a promising source of radiation for remote DIAL-DOAS sounding of the TAGs under study along surface tropospheric paths. The laser system design provides for a possibility of narrowing the lasing line within the  $0.01\text{--}5\text{ cm}^{-1}$  limits. This possible improvement along with a small step of lasing line tuning and the presence of absorption lines of other atmospheric gases, including atmospheric pollutants, in the spectral range under consideration make this laser a unique instrument for designing a ground-based DIAL lidar.

## 6. ACKNOWLEDGMENTS

The work was supported by the Russian Science Foundation (Agreement no. 14-27-00022).

## REFERENCES

1. Vasil'ev, B.I. and Mannoun, U.M., IR differential-absorption lidars for ecological monitoring of the environment, *Quantum Electron*, 2006, vol. 36, no. 9, pp. 801–820.
2. Mitev, V., Babichenko, S., Bennes, J., et al., Mid-IR DIAL for high-resolution mapping of explosive precursors, *Proc. SPIE*, 2013, vol. 8894, 88940S.
3. Burlakov, V.D., Dolgii, S.I., Nevzorov, A.A., Nevzorov, A.V., and Romanovskii, O.A., Algorithm for retrieval of vertical distribution of ozone from DIAL laser remote measurements, *Optical Memory and Neural Networks (Information Optics)*, 2015, vol. 24, no. 4, pp. 295–302.
4. Sunesson, J.A., Apituley, A., and Swart, D.P., Differential absorption lidar system for routine monitoring of tropospheric ozone, *Applied Optics*, 1994, vol. 33, no. 30, pp. 7045–7058.
5. Browell, E.V., Differential absorption lidar sensing of ozone, *Proc. IEEE*, 1989, vol. 77, no. 3, pp. 419–432.
6. McGee, T.J., Gross, M., Singh, U.N., et al., Improved stratospheric ozone lidar, *Optical Engineering*, 1995, vol. 34, no. 5, pp. 1421–1430.
7. Higdón, N.S., Browell E.V., Ponsardin, P., et al., Airborne differential absorption lidar system for measurements of atmospheric water vapor and aerosols, *Applied Optics*, 1994, vol. 33, no. 27, pp. 6422–6438.
8. Toriumi, R., Tai, H., and Takeuchi, N., Tunable solid-state blue laser differential absorption lidar system for NO<sub>2</sub> monitoring, *Optical Engineering*, 1996, vol. 35, no. 8, pp. 2371–2375.
9. Romanovskii, O.A., Kharchenko, O.V., and Yakovlev, S.V., Application of multiwavelength IR lasers for lidar and path measurements of the meteorological parameters of the atmosphere, *Rus. Phys. J.*, 2015, vol. 57, no. 10, pp. 1380–1387.
10. Platt, U., Perner, D., and Patz, H.W., Simultaneous measurement of atmospheric CH<sub>2</sub>O, O<sub>3</sub>, and NO<sub>2</sub> by differential optical-absorption, *J. Geophys. Res.*, 1979, vol. 84, pp. 6329–6335.
11. Platt, U., Differential optical absorption spectroscopy (DOAS), *Air Monitoring by Spectroscopic Techniques. Chemical Analysis Series*, 1994, vol. 127, pp. 27–84.
12. Platt, U. and Stutz, J., *Differential Optical Absorption Spectroscopy*, New-York, Berlin, Heidelberg: Springer-Verlag, 2008, p. 593.
13. Douard, M., Bacis, R., Rambaldi, P., et al., Fourier-transform lidar, *Optics Letters*, 1995, vol. 20, no. 20, pp. 2140–2143.